2005 American Control Conference
June 8-10, 2005. Portland, OR, USA

Underwater Navigation In the Presence of Unknown Currents Based On Range Measurements From a Single Location

Aditya S. Gadre Daniel J. Stilwell
The Bradley Department of Electrical and Computer Engineering
Virginia Polytechnic Institute and State University
Blacksburg, VA 24061
{*agadre, stilwell*}@*vt.edu*

***Abstract*— An underwater navigation algorithm is considered that enables an underwater vehicle to compute its trajectory in the presence of unknown currents by utilizing range measurements from a single known location. There exists a small set of trajectories for which the algorithm does not converge. By assessing local observability about potential vehicle trajectories, we characterize those trajectories that cannot be asymptotically estimated. The navigation algorithm is illustrated using computer simulation and a hardware experiment.**

I. Introduction

The concept of underwater navigation using range measurements from a single known location is motivated by the needs of small autonomous underwater vehicles, such as those described in [1] and [2]. Traditional navigation technologies, such as long-base-line (LBL) and high accuracy inertial navigation systems, are prohibitively difficult to use for small vehicles due to power and volume constraints. Navigation based on range measurements from a single source has the potential to reduce both hardware complexity and deployment time, and it may enable other navigation objectives, such as navigation of small AUVs relative to a larger AUV. Underwater navigation based on range measurements from a single source has also been considered in [3] and [4], in which other potential uses are discussed, such as multiple vehicle operations including leader-follower formations and large area surveys. The authors have previously considered underwater navigation in the presence of currents in [5], in which it was assumed that underwater currents were known. The principal contribution of this work is to show that unknown currents can be identified along with the AUV's position.

As is standard for navigation algorithms, the system dynamics utilized herein are based on a kinematic model of the AUV. Further we assume that currents are constant. By assuming a kinematic model, there will be a mismatch between the estimated and true motion of the AUV during turning motions. A kinematic model does not capture the side-slip motion during turning of a streamlined AUV with tail fin control surfaces. This results in bounded position estimation errors along turns, but errors converge to zero along straight-line trajectories. Similarly, the kinematic model does not account for the inertial effects of time-varying currents on the vehicle motion. These effects would be noticeable when the AUV enters an area where the currents have a different direction or a different speed. Thus the estimation algorithm experiences bounded errors during turns and when the change in currents is not appreciably slower than the estimation time constant. Our field experiments have shown that position estimation error does increase when the current direction changes relative to the AUV's trajectory, but converges when currents are constant.

II. Problem statement

An underwater vehicle can determine its range from an acoustic beacon using time-of-flight of an acoustic pulse. Without loss of generality, absolute position of the acoustic beacon is assumed to be (0, 0). Since the z-axis of an underwater vehicle is easily instrumented using a depth sensor, we simplify notation and consider motion only in the horizontal plane. The AUV trajectory is denoted by $p(t) = [x(t), y(t)]^T$, where $x(t)$ and $y(t)$ are position coordinates. We assume the presence of constant currents whose magnitude v_c and direction φ_c are unknown. We treat v_c and φ_c as system parameters to be estimated and augment the state vector with them. The kinematic equations of motion are

$$\begin{bmatrix} \dot{x}(t) \\ \dot{y}(t) \\ \dot{\varphi}(t) \\ \dot{v_c}(t) \\ \dot{\varphi}_c(t) \end{bmatrix} = \begin{bmatrix} u_1(t)\cos\varphi(t) + v_c\cos\varphi_c \\ u_1(t)\sin\varphi(t) + v_c\sin\varphi_c \\ u_2(t) \\ 0 \\ 0 \end{bmatrix} \qquad (1)$$

$$h(t) = \begin{bmatrix} \sqrt{x^2(t) + y^2(t)} \\ \varphi(t) \end{bmatrix}$$

where $u_1(t)$ is the speed of the vehicle in the direction of heading $\varphi(t)$, $u_2(t)$ is the rate of change of $\varphi(t)$ and $h(t)$ is the measured output of the system. The range of the vehicle from the origin is

$$r(t) = \|p(t)\| = \sqrt{x^2(t) + y^2(t)}$$

Assuming $r(t) > 0$ for all t, the nonlinear system in (1) can be transformed into the polar coordinates

$$\begin{bmatrix} \dot{r}(t) \\ \dot{\theta}(t) \\ \dot{\varphi}(t) \\ \dot{v_c}(t) \\ \dot{\varphi}_c(t) \end{bmatrix} = \begin{bmatrix} u_1(t)\cos(\varphi(t)-\theta(t)) + v_c\cos(\varphi_c-\theta(t)) \\ \frac{u_1(t)}{r(t)}\sin(\varphi(t)-\theta(t)) + \frac{v_c}{r(t)}\sin(\varphi_c-\theta(t)) \\ u_2(t) \\ 0 \\ 0 \end{bmatrix}$$
$$h(t) = \begin{bmatrix} r(t) \\ \varphi(t) \end{bmatrix},\ r(t) > 0\ \forall t \in [t_0, t_f] \tag{2}$$

where $\theta(t) = \text{ATAN2}(y(t), x(t))$. Polar coordinates will be used in the sequel for assessing observability.

III. Observability Analysis

It has been shown in [6] that local observability is sufficient for existence of an observer that displays asymptotically stable error dynamics, if the estimate of the initial state is sufficiently close to the true initial state. In this section, conditions are identified under which the nonlinear system (2) is locally observable. Local observability is assessed by linearizing the kinematic model about arbitrary trajectories and studying observability of the linearized system.

A linear time-varying system is obtained by linearizing the nonlinear system (2) around a nominal trajectory.

$$\begin{aligned} \dot{s_\delta}(t) &= A(t)s_\delta(t) + B(t)u_\delta(t),\ s_\delta(0) = s_{\delta 0},\ ,\ t \in [t_o, t_f] \\ h_\delta(t) &= C(t)s_\delta(t), \end{aligned} \tag{3}$$

where

$$A(t) = \begin{bmatrix} 0 & A_{12}(t) & A_{13}(t) & A_{14}(t) & A_{15}(t) \\ A_{21}(t) & A_{22}(t) & A_{23}(t) & A_{24}(t) & A_{25}(t) \\ 0 & 0 & 0 & 0 & 0 \\ 0 & 0 & 0 & 0 & 0 \\ 0 & 0 & 0 & 0 & 0 \end{bmatrix}$$

where

$$\begin{aligned} A_{12}(t) &= u_1(t)\sin\beta(t) + v_c\sin\gamma(t) \\ A_{13}(t) &= -u_1(t)\sin\beta(t) \\ A_{14}(t) &= \cos\gamma(t) \\ A_{15}(t) &= -v_c\sin\gamma(t) \\ A_{21}(t) &= -\frac{u_1(t)}{r^2(t)}\sin\beta(t) - \frac{v_c}{r^2(t)}\sin\gamma(t) \\ A_{22}(t) &= -\frac{u_1(t)}{r(t)}\cos\beta(t) - \frac{v_c}{r(t)}\cos\gamma(t) \\ A_{23}(t) &= \frac{u_1(t)}{r(t)}\cos\beta(t) \\ A_{24}(t) &= \frac{\sin\gamma(t)}{r} \\ A_{25}(t) &= \frac{v_c\cos\gamma(t)}{r} \end{aligned}$$

$$B(t) = \begin{bmatrix} \cos(\beta) & 0 \\ \frac{1}{r(t)}\sin\beta(t) & 0 \\ 0 & 1 \\ 0 & 0 \\ 0 & 0 \end{bmatrix},\quad C(t) = \begin{bmatrix} 1 & 0 & 0 & 0 & 0 \\ 0 & 0 & 1 & 0 & 0 \end{bmatrix}$$

where $\beta(t) = \varphi(t) - \theta(t), \quad \gamma(t) = \varphi_c - \theta(t)$

For observability analysis of the linearized system (3), we use a standard rank test for the observability of time varying linear systems (see e.g. [7], pp. 149).

Lemma 3.1: Suppose $q \leq (n-1)$ is a positive integer such that $C(t)$ is at least q times continuously differentiable, and $A(t) \in \mathbb{R}^{n\times n}$ is $q-1$ times continuously differentiable. Then the linear system is observable on time interval $[t_o, t_f]$, if for some $t \in [t_o, t_f]$, $\operatorname{rank} O(t) = n$, where,

$$\begin{aligned} O(t) &= \begin{bmatrix} L_0(t) \\ \vdots \\ L_q(t) \end{bmatrix} \\ L_0(t) &= C(t) \\ L_j(t) &= L_{j-1}(t)A(t) + \dot{L}_{j-1}(t) \end{aligned} \tag{4}$$

If the linearized system is observable over time interval $[t_o, t_f]$, then the nonlinear system is locally observable over that time interval.

We find conditions under which a trajectory is observable. These conditions are in terms of $\dot{\theta}(t)$. It turns out that unlike in [5], the set of unobservable trajectories is not trivial. It is also important to note that the system is not observable if $v_c = 0$. The case where $v_c = 0$ is addressed in [5]. Development of an algorithm that satisfies both cases is a subject of further research.

Theorem 3.2: Assume $u_1(t) \neq 0$ and $v_c \neq 0$ for all $t \in [t_o, t_f]$. Then the linearized system (3) is observable over the time interval $[t_o, t_f]$ if

$$\dot{\theta}(t) \neq \frac{4a^3}{4a^2 - 4ab\,(t-t_0) + (4a^4 + b^2)\,(t-t_0)^2}$$

for some $t \in [t_o, t_f]$, where $a = \dot{\theta}(t_0)$ and $b = \ddot{\theta}(t_0)$.

Proof: The observability matrix $O(t)$ for the linearized system (3) is

$$O(t) = \begin{bmatrix} 1 & 0 & 0 & 0 & 0 \\ 0 & 0 & 1 & 0 & 0 \\ 0 & O_{32}(t) & O_{33}(t) & O_{34}(t) & O_{35}(t) \\ 0 & 0 & 0 & 0 & 0 \\ O_{51}(t) & O_{52}(t) & O_{53}(t) & O_{54}(t) & O_{55}(t) \\ 0 & 0 & 0 & 0 & 0 \\ O_{71}(t) & O_{72}(t) & O_{73}(t) & O_{74}(t) & O_{75}(t) \\ 0 & 0 & 0 & 0 & 0 \end{bmatrix} \tag{5}$$

where

$$
\begin{aligned}
O_{32}(t) &= \dot{\theta}(t) r(t) \\
O_{33}(t) &= -u_1(t) \sin\beta(t) \\
O_{34}(t) &= \cos\gamma(t) \\
O_{35}(t) &= -v_c \sin\gamma(t) \\
O_{51}(t) &= -\dot{\theta}^2(t) \\
O_{52}(t) &= \ddot{\theta}(t) r(t) \\
O_{54}(t) &= 2\dot{\theta}(t) \sin\gamma(t) \\
O_{55}(t) &= 2v_c \dot{\theta}(t) \cos\gamma(t) \\
O_{71}(t) &= -3\dot{\theta}(t)\ddot{\theta}(t) \\
O_{72}(t) &= -\dot{\theta}^3(t) r(t) + \dddot{\theta}(t) r(t) \\
O_{74}(t) &= -3\dot{\theta}^2(t) \cos\gamma(t) + 3\ddot{\theta}(t) \sin\gamma(t) \\
O_{75}(t) &= 3v_c \dot{\theta}^2(t) \sin\gamma(t) + 3v_c \ddot{\theta}(t) \cos\gamma(t)
\end{aligned}
$$

Assume that the linearized system (3) is not observable over the entire time interval $[t_o, t_f]$. Then by Lemma 3.1, $O(t)$ is not full rank for all $t \in [t_o, t_f]$. Since columns 1 and 3 are independent of each other, the 3x3 sub-matrix

$$
\bar{O}(t) = \begin{bmatrix} \dot{\theta}(t) r(t) & \cos\gamma(t) & -v_c \sin\gamma(t) \\ \ddot{\theta}(t) r(t) & 2\dot{\theta}(t) \sin\gamma(t) & 2v_c \dot{\theta}(t) \cos\gamma(t) \\ -\dot{\theta}^3(t) r(t) + \dddot{\theta}(t) r(t) & O_{74}(t) & O_{75}(t) \end{bmatrix} \tag{6}
$$

obtained from $O(t)$ by removing columns 1 and 3 and all rows with all elements zero, must be rank deficient for all $t \in [t_o, t_f]$. This means

$$
\det \bar{O}(t) = 0 \quad \forall t \in [t_o, t_f]
$$

We can therefore write, for all $t \in [t_o, t_f]$,

$$
4v_c r(t) \dot{\theta}^4(t) - 3v_c r(t) \ddot{\theta}^2(t) + 2v_c r(t) \dot{\theta}(t) \dddot{\theta}(t) = 0 \tag{7}
$$

Since $v_c \neq 0$ and $r(t) \neq 0$ for all $t \in [t_o, t_f]$, (7) is equivalent to

$$
4\dot{\theta}^4(t) - 3\ddot{\theta}^2(t) + 2\dot{\theta}(t) \dddot{\theta}(t) = 0, \ \ \forall t \in [t_o, t_f] \tag{8}
$$

Solving the differential equation in (8) for $\dot{\theta}(t)$, we can write

$$
\dot{\theta}(t) = \frac{4a^3}{4a^2 - 4ab\,(t - t_0) + (4a^4 + b^2)\,(t - t_0)^2} \tag{9}
$$

where $a = \dot{\theta}(t_0)$ and $b = \ddot{\theta}(t_0)$. Thus if the linearized system (3) is not observable then

$$
\dot{\theta}(t) = \frac{4a^3}{4a^2 - 4ab\,(t - t_0) + (4a^4 + b^2)\,(t - t_0)^2} \tag{10}
$$

for all $t \in [t_o, t_f]$. Invoking the contrapositive yields the desired result. ∎

In general, it should be easy for an AUV to avoid the unobservable trajectories described by (9). There is at least one unobservable trajectory that is easily described.

Theorem 3.3: Straight line trajectories passing through the origin are not locally observable.

Proof: For straight line trajectories passing through the origin, we can write $\dot{\theta}(t) = 0$ for all $t \in [t_0, t_f]$. Hence from (2) we can write

$$
u_1(t) \sin(\varphi(t) - \theta(t)) + v_c \sin(\varphi_c - \theta(t)) = 0
$$

Substituting in (3)

$$
A(t) = \begin{bmatrix} 0 & 0 & A_{13}(t) & A_{14}(t) & A_{15}(t) \\ 0 & A_{22}(t) & A_{23}(t) & A_{24}(t) & A_{25}(t) \\ 0 & 0 & 0 & 0 & 0 \\ 0 & 0 & 0 & 0 & 0 \\ 0 & 0 & 0 & 0 & 0 \end{bmatrix}
$$

Also since $\dot{\theta}(t) = 0$ for all $t \in [t_0, t_f]$, $\dot{\varphi}(t) = 0$ for all $t \in [t_0, t_f]$. $B(t)$ and $C(t)$ are the same as in (3). The observability matrix $O(t)$ for this system is

$$
O(t) = \begin{bmatrix} 1 & 0 & 0 & 0 & 0 \\ 0 & 0 & 1 & 0 & 0 \\ 0 & 0 & -u_1(t) \sin\beta(t) & \cos\gamma(t) & -v_c \sin\beta(t) \\ 0 & 0 & 0 & 0 & 0 \\ 0 & 0 & 0 & 0 & 0 \\ 0 & 0 & 0 & 0 & 0 \\ 0 & 0 & 0 & 0 & 0 \\ 0 & 0 & 0 & 0 & 0 \end{bmatrix}
$$

Thus $O(t)$ is rank deficient for all $t \in [t_o, t_f]$, with $\operatorname{rank} O(t) = 3$. Therefore by Lemma 3.1, the linearized system is not observable when $\dot{\theta}(t) = 0$ for all $t \in [t_o, t_f]$ and hence straight line trajectories passing through origin are not locally observable. ∎

IV. Observer error dynamics

Observability conditions derived in Section III are sufficient for the observability grammian to be invertible, and equivalently for the initial condition to be uniquely determined from the measured output and the input. However, they are not sufficient for the existence of a Luenberger observer with error dynamics that are bounded by a decaying exponential over an interval. Modest restatement of [7] (pp. 267) provides the required connection between observability and exponentially decaying observation error dynamics.

Lemma 4.1: Suppose there exists $\delta > 0$ such that the linear system (3) is observable over the intervals $[t - \delta, t]$ for all $t \in [t_o + \delta, t_f]$, then there exists an observer gain such that the error-state of a Luenberger observer decays exponentially over the interval $[t_o, t_f]$.

Combining the specific observability requirements for navigation from Theorem 3.2 with the existence conditions for an observer gain in Lemma 4.1 yields specific conditions on the trajectory of an AUV for which a Luenberger observer exists, at least for the interval $[t_o + \delta, t_f]$.

Theorem 4.2: Suppose $u_1(t) \neq 0$ and $v_c \neq 0$ for all $t \in [t_0, t_f]$. Then there exists an observer gain such that the

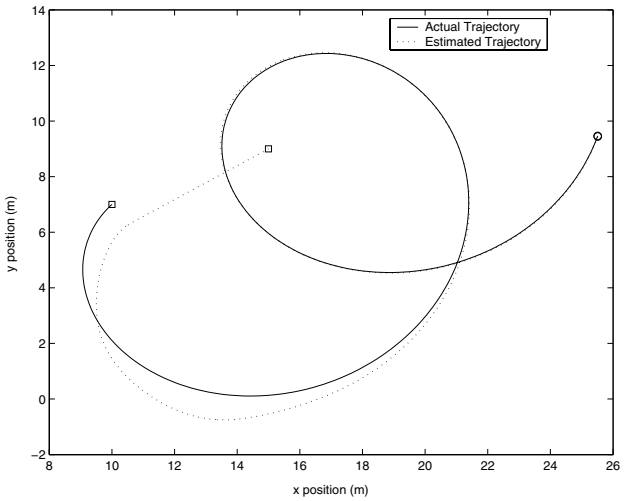

Fig. 1. Observable spiral trajectory in the presence of unknown currents. Squares indicate start points.

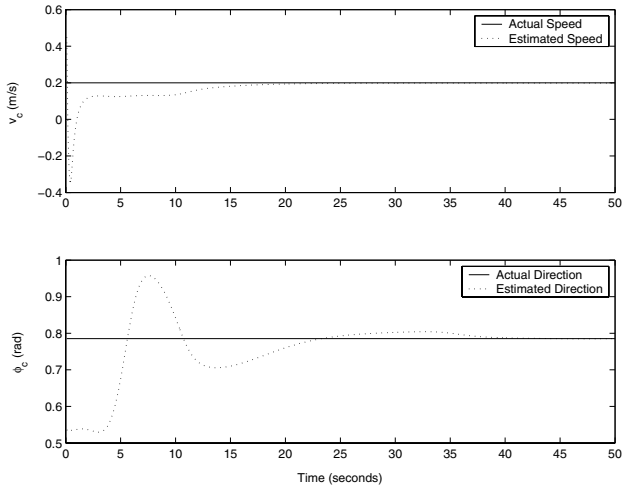

Fig. 2. Actual and estimated current magnitude and direction for a spiral trajectory.

error-state of a Luenberger observer decays exponentially if there exists $\delta > 0$ such that

$$\dot{\theta}(t) \neq \frac{4\dot{\theta}^3(\tau)}{4\dot{\theta}^2(\tau) - 4\dot{\theta}(\tau)\ddot{\theta}(\tau)\delta + \left[4\dot{\theta}^2(\tau) + \ddot{\theta}^2(\tau)\right]\delta^2} \quad (11)$$

for all $t \in [t_o + \delta, t_f]$, where $\tau = t - \delta$.

The case of a straight-line trajectory passing through the origin, for which $\dot{\theta}(t) = 0$ and $\ddot{\theta}(t) = 0$ for all t, is not covered by Theorem 4.2. Instead, recalling Theorem 3.3 we conclude the following.

Theorem 4.3: For straight-line trajectories passing through the origin, there exists no observer gain such that a Luenberger observer has error-states that decay exponentially.

Under the restrictions on an AUV's trajectory provided by Theorems 4.2 and 4.3, a navigation algorithm can be implemented using a Luenberger observer. However, navigation algorithms are commonly implemented with a Kalman filter. We also do this in Section V. Loosely speaking for the sake of brevity, a Kalman filter requires observability over the family of intervals $[t - \delta, t]$ as we have shown, along with controllability of the pair $[A(t), G(t)]$ where $G(t)$ is the coefficient matrix for an assumed process noise [8], [9]. In practice, this additional controllability requirement is achieved for standard assumptions on $G(t)$.

V. Simulation results in the presence of unknown currents

In this section, simulation results are presented using trajectories that are generated by the kinematic model with non-zero currents and an extended Kalman filter for estimation. Figure 1 shows a locally observable trajectory with $v_c = 0.2$ m/s, $\varphi_c = \pi/4$ radians, $u_1 = 1$ m/s and $u_2 = 0.025$ rad/s. Figure 2 shows actual and estimated magnitude and direction of the current.

VI. Experiment

The navigation algorithm is demonstrated using representative hardware, but without building or otherwise acquiring the acoustic hardware required to compute underwater range from a known location. A miniature AUV, developed at Virginia Tech [2], was deployed in the Lafayette river near Norfolk, Virginia. Tidal flow produces significant currents in the river. The AUV was run on the surface so that GPS signals were available continuously. Position information from GPS was used to compute range from a fixed location and provide ground truth for the algorithm. The AUV was instrumented with an electronic compass for measuring heading $\varphi(t)$ and an MEMS gyro for measuring angular rate $u_2(t)$. Propeller position of the AUV was instrumented, enabling estimates of AUV water-relative speed $u_1(t)$ from steady-state propeller rotation rate. Currents were measured using three drifters, designed by Dr. Jay Austin of the Old Dominion University [10]. Drifters read their GPS positions as they drift along with currents. GPS data from the drifters was then used to calculate current speed and direction. Due to sensor noise and uncertainties, we believe this experimental platform provides a reasonably realistic hardware experiment of the navigation algorithm.

The AUV trajectory, obtained by the on-board GPS, is in the Latitude-Longitude-Altitude (LLA) format. It is converted into a planar trajectory by transforming it into Earth-Fixed (EF) coordinate frame, whose origin is set to a known location. GPS data from the drifters is also converted into the same EF frame. Figure 3 shows trajectories of the AUV and the drifters. The positive x-axis points due East and positive y-axis points due North. The range $r(t)$ of the AUV from the known location (the origin) is computed as $r(t) = \sqrt{x^2(t) + y^2(t)}$, where $x(t)$ and $y(t)$ are East and North position coordinates of the AUV with respect to the origin. AUV heading $\varphi(t)$ obtained from an electronic compass is shown in Figure 4. Compass measurements are

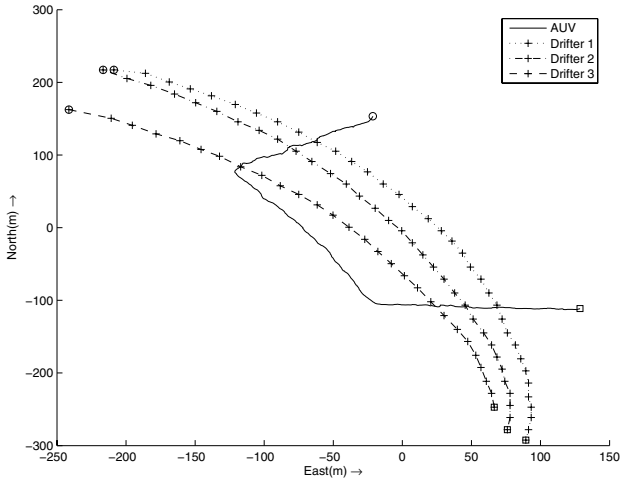

Fig. 3. AUV and drifter trajectories. Squares and circles denote start and end points respectively. '+' indicates points where each drifter collected GPS data. At each of these points, current speed and direction are computed.

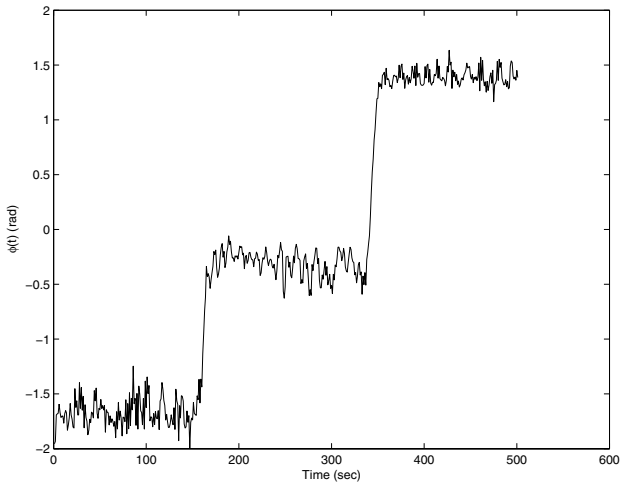

Fig. 4. AUV heading $\varphi(t)$ obtained from compass.

with respect to the true North. Figure 5 shows corresponding angular rate $u_2(t)$ obtained from an MEMS rate gyro. Current speed and direction are computed from drifters GPS data. As can be seen in Figure 3, current direction varies spatially. Current speed and direction along the AUV trajectory are thus not constant. At any point (x, y) current speed and direction are approximated by the speed and direction at the nearest drifter data point.

An extended Kalman filter (EKF) based on the kinematic model (1) is implemented to estimate the AUV position and current speed and direction. EKF implementation is standard (see e.g. [11], pp. 496), except we assume that the process noise covariance $Q(k)$ varies with time. When AUV is making a turn we assume it to be higher than that when the AUV is moving along a straight line, to account for the fact that along a turn kinematic equations model AUV motion less accurately due to non-zero angle of attack.

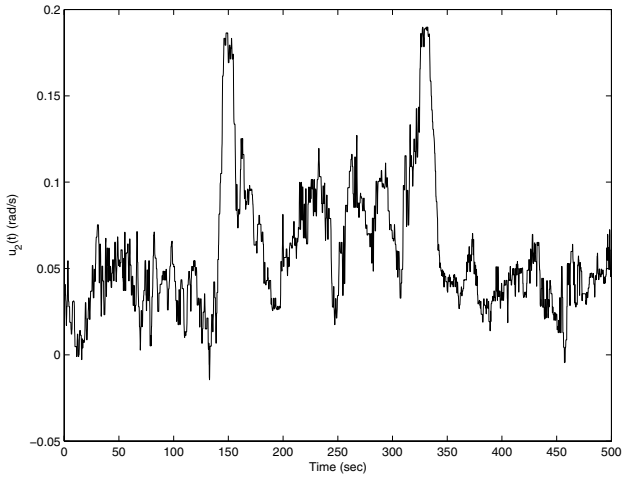

Fig. 5. AUV angular rate $u_2(t)$ obtained from MEMS gyro.

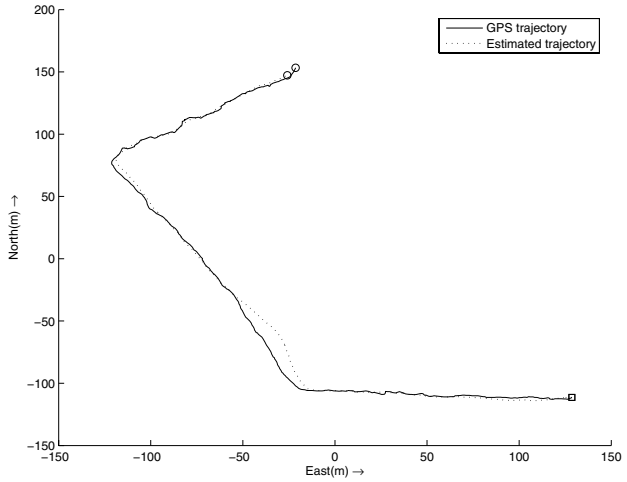

Fig. 6. Actual and estimated trajectories. Squares and circles indicate start and end points respectively.

A. Results

Figure 6 shows actual trajectory obtained by the GPS and the trajectory estimated by the EKF. Figure 7 shows actual and estimated position coordinates and actual and estimated AUV headings. Figure 8 shows actual and estimated current speed and direction along the AUV trajectory. The position estimate diverges from the actual position along turns. This is due to mismatch between the kinematic model of AUV motion and the actual AUV dynamics during turning maneuvers [5]. The estimated trajectory converges to the actual trajectory after the turning maneuver, along straight line legs of the trajectory.

It is important to note that the kinematic equations of the AUV motion assume constant speed and direction of currents. Despite this, the EKF could track changes in the current direction φ_c. We believe if these variables change slowly, then the estimation errors induced by changing currents are negligible.

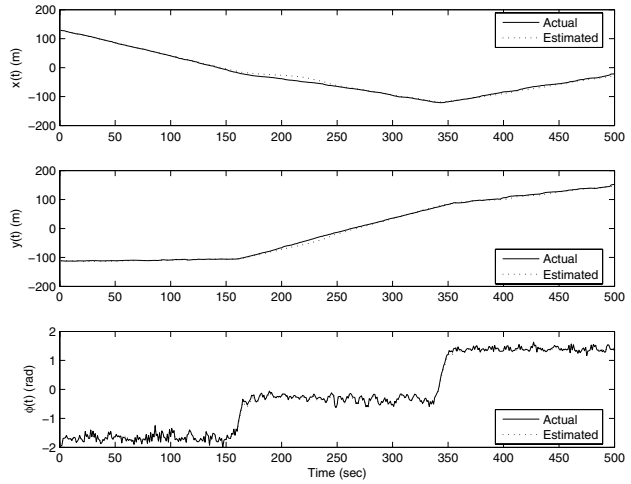

Fig. 7. Actual and estimated AUV position coordinates $x(t)$ and $y(t)$ and AUV heading $\varphi(t)$.

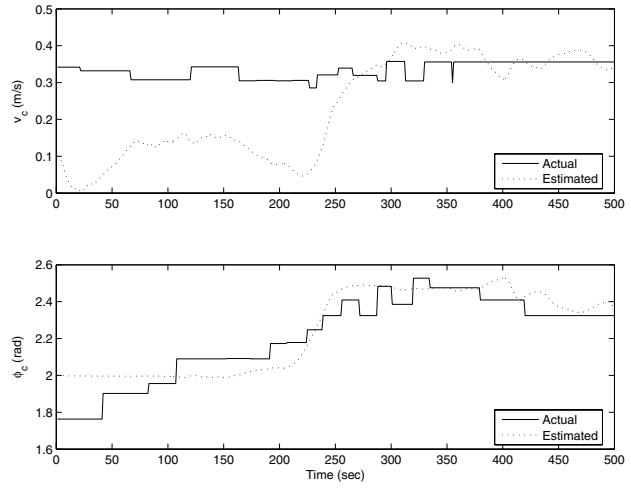

Fig. 8. Actual and estimated current speed v_c and direction φ_c.

VII. Conclusion and Future work

A navigation algorithm has been proposed that is potentially suitable for very small AUVs in the presence of unknown currents. The algorithm requires range measurements from a known location, heading from a compass, yaw-rate from a MEMS gyro, and advance velocity from steady-state propeller rotation rate. The principal contribution of this work is a precise observability analysis that characterizes locally observable trajectories in the presence of unknown currents.

We have shown through local observability analysis that currents can be successfully estimated at the same time the AUV trajectory is estimated. This fact is demonstrated by simulation studies and hardware experiment in real world deployment. This would enable AUVs to navigate based on range measurements from a single location even when there are unknown non-zero currents. It is also shown through hardware experiment that if current parameters vary slowly, the estimation errors due to these variations are negligible and the navigation algorithm can track these variations in real time.

Acknowledgment

The authors are extremely grateful for the support of Dr. Jay Austin at the Center for Coastal Physical Oceanography, Old Dominion University, who supplied drifters for the experiment and participated in all field operations. Authors gratefully acknowledge the support of National Science Foundation via grant IIS-0238092, Office of Naval Research via grant N00014-03-1-0444.

References

[1] B. Hobson, B. Schulz, J. Janet, M. Kemp, R. Moody, C. Pell, and H. Pinnix, "Development of a micro autonomous underwater vehicle for complex 3-D sensing," in *Proceedings of the IEEE/MTS OCEANS*, 2001, pp. 2043–2045.

[2] A. Gadre, J. E. Mach, D. J. Stilwell, and C. E. Wick, "A prototype miniature autonomous underwater vehicle," in *Proceedings of IEEE/RSJ International Conference on Intelligent Robots and Systems*, Las Vegas, NV, November 2003.

[3] J. Vaganay, P. Baccou, and B. Jouvencel, "Homing by acoustic ranging to a single beacon," in *Proceedings of the OCEANS 2000 MTS/IEEE Conference and Exhibition*, Providence, RI, September 2000, pp. 1457–1462.

[4] P. Baccou and B. Jouvencel, "Simulation results, post-processing experimentation and comparison results for navigation, homing and multiple vehicle operations with a new positioning method using a transponder," in *Proceedings of the 2003 IEEE/RSJ International Conference on Intelligent Robots and Systems*, Las Vegas, NV, October 2003, pp. 811–817.

[5] A. Gadre and D. J. Stilwell, "Toward underwater navigation based on range measurements from a single location," in *Proceedings of IEEE International Conference on Robotics and Automation*, New Orleans, LA, April 2004.

[6] T. L. Song, "Observability of target tracking with range-only measurements," *IEEE J. Oceanic Eng.*, vol. 24, no. 3, pp. 383–387, July 1999.

[7] W. J. Rugh, *Linear Systems Theory*, 2nd ed. London, United Kingdom: Prentice Hall Publications, 1996.

[8] R. E. Kalman and R. S. Bucy, "New results in linear filtering and prediction theory," *ASME Journal of Basic Engineering*, vol. 83, pp. 95–108, Mar. 1961.

[9] R. E. Kalman, "New methods in wiener filtering theory," *Proceedings of Symposium on Eng. Appl. Random Function Theory and Probability*, pp. 270–388, 1963.

[10] J. Austin and S. Atkinson, "The design and testing of small, low-cost GPS-tracked surface drifters," *To be published in Estuaries*, 2004.

[11] S. Haykin, *Adaptive Filter Theory*, 4th ed. Upper Saddle River, New Jersy, USA: Prentice Hall Publications, 2002.